

Seasonal climate summary southern hemisphere (summer 1999/2000): a second successive weak cool episode (La Niña) reaches maturity

Paul M. Della-Marta

National Climate Centre, Bureau of Meteorology, Australia

(Manuscript received December 2000)

Southern hemisphere atmospheric and oceanic patterns for summer 1999/2000 are reviewed, with emphasis given to the tropical Pacific Ocean and the Australian region. A second successive cool phase in the equatorial Pacific reached maturity by mid-summer. The atmosphere lagged, with an enhanced Walker circulation reaching its peak by the end of summer. A large pool of warmer than normal water remained in the western equatorial Pacific. In the Australian region, warm SSTs surrounded most of the continent, the only exception being parts of the east coast. Very warm SSTs were located along, and to the southwest of the Western Australian coast.

Centres of anomalously high mean sea-level pressure were well south of their climatological positions, with Australia dominated by moist monsoonal northerly flow. Areas of cyclonicity developed off both the northwest and northeast coasts throughout summer. These were most marked in the west in December, and in the northeast later in the season. In general, wet and cool conditions occurred over most of the continent. The Australian average summer rainfall was the third highest on record, surpassed only by the distinctly wet mid-1970s La Niña events. Western Australia experienced its wettest summer on record and during the 1990s has recorded four out of the ten wettest summers on record. Exceptions were a dry eastern New South Wales and a warm west coast and southern eastern Australia.

Introduction

Atmospheric and oceanic indicators of the El Niño – Southern Oscillation (ENSO) for summer 1999/2000 suggested a second successive cool phase (La Niña) had reached maturity. This event was preceded by one

of similar strength during the summer 1998/1999 (Trewin 1999), followed by a phase of neutral conditions and signs of redevelopment in spring 1999 (de Hoedt 2000; Jones 2000; Watkins 2000). The SOI for summer 1999/2000 was +10.3. The central (western) equatorial Pacific Ocean showed a strong cooling (warming) trend over summer. Low-level central Pacific Ocean equatorial easterly winds strengthened and outgoing long wave radiation showed a continued positive

Corresponding Author Address: Paul M. Della-Marta, National Climate Centre, Bureau of Meteorology, GPO Box 1289K, Melbourne, Vic. 3001, Australia.

Email: P.Della-Marta@bom.gov.au

trend in the western Pacific, both indicators of an enhanced Walker circulation. By midsummer eastern equatorial subsurface analyses showed signs of warming, foreshadowing the decay of the La Niña event. Over Australia, the distributions of rainfall and temperature anomalies were consistent with an ENSO cool phase (Jones and Trewin 2000), with above average rainfall and cool temperatures over most of the continent.

Data

The main sources of information used for this summary were the *Climate Monitoring Bulletin* (Bureau of Meteorology, Melbourne, Australia) and the *Climate Diagnostics Bulletin* (Climate Prediction Centre, Washington D.C., USA). Data sources are given in the Appendix.

Pacific basin climate indices

The Southern Oscillation Index (SOI)*

After the rapid rise of the SOI in spring 1999 (Watkins 2000) the SOI for summer 1999/2000 remained positive with a mean value of +10.3. Individual SOI values for December, January and February were +12.8, +5.1 and +12.9 respectively (Fig. 1).

Over the summer period mean sea-level pressure (MSLP) anomalies at Darwin increased from a value of -0.7 hPa in December to 0.0 hPa by the end of February. The MSLP anomaly at Tahiti remained positive, strengthening to +2.7 hPa by February. The lower January SOI, +5.1, was due to both an increase in the Darwin MSLP and a reduction in Tahiti MSLP. A large anticyclonic MSLP anomaly south of eastern Australia (Fig. 7) was persistent throughout summer, and during January, a ridge formed over the eastern half of the continent having an influence on the Darwin MSLP readings.

Outgoing long wave radiation (OLR)

The time series from January 1996 to February 2000 of monthly standardised outgoing long wave radiation anomalies for the region from 5°N to 5°S, 160°E to 160°W, is shown in Fig. 2. These data were provided by the Climate Prediction Centre, Washington D.C. (CPC 2000). Negative values of the OLR index suggest cooler black body temperatures, which tend to be associated with an increase in high cloud and hence convection, and, as a result may also signal increased rainfall.

Fig. 1 Southern Oscillation Index, January 1996 to February 2000 inclusive. Means and standard deviations based on the period 1933-92.

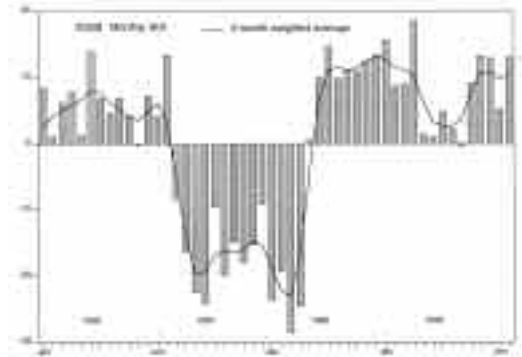
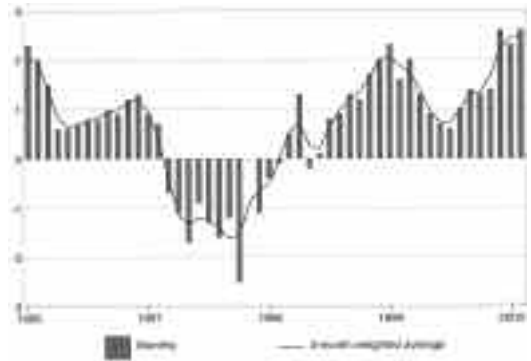


Fig. 2 Standardised anomaly of monthly outgoing long wave radiation averaged over 5°N-5°S and 160°E-160°W, for January 1996 to February 2000. Negative (positive) anomalies indicate enhanced (reduced) convection and rainfall. Anomalies are based on a 1979-95 base period of mean. After CPC (1999).



During summer positive OLR anomalies strengthened, a sign of decreased convection in the central western tropical Pacific (Fig. 2). In contrast to the spring mean OLR anomaly of +1.4 (Watkins 2000), summer had an average of +2.5. The December and February value of this index was +2.6, which is the second highest value in the historical record dating back to 1974, surpassed only by the December 1975 value (CPC 1999, 2000). These anomalies are associated with cooler than average sea-surface temperatures in this region and suggest an enhanced Walker circulation. In the Australian region the OLR anomalies (not shown) became increasingly negative over

* The SOI used here is ten times the monthly anomaly of the difference in mean sea-level pressure between Tahiti and Darwin, divided by the standard deviation of that difference for the relevant month, based on the period 1933-92.

the northern half of the continent throughout summer. A significant negative anomaly covered the western half of the continent in January, the result of an enhanced west coast trough and its interaction with a tropical low off the northwest coast. By February widespread negative OLR anomalies existed over Southeast Asia and in a line from northern Australia to the central Indian Ocean. The rise of monsoon activity over northern Australia throughout summer is also demonstrated with monthly maps of the 200 hPa velocity potential (not shown), a measure of upper level divergence. Centres of negative velocity potential over Indonesia and the Coral Sea merged to form one centre of negative anomaly over northern Australia by late summer.

Ocean patterns

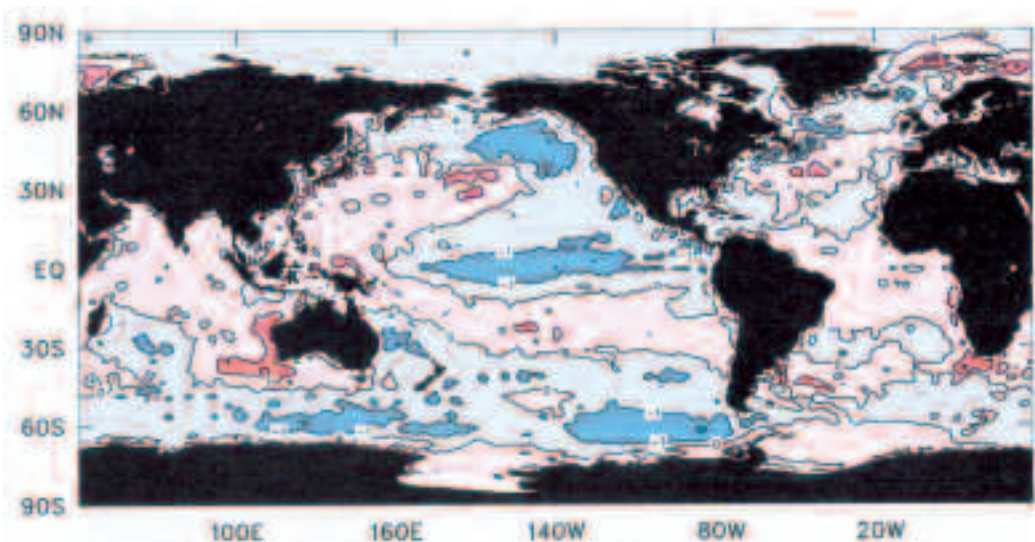
Sea-surface temperature (SST) patterns

The mean summer SST anomaly distribution (Fig. 3) shows a significant cooling in the central equatorial Pacific compared with the previous season (Watkins 2000), and a clear re-establishment of La Niña conditions. A large pool of cooler than average equatorial SSTs extended from 170°E to 110°W, between 10°N and 5°S. Anomalies in this area are generally between -1°C and -2°C with -2°C being exceeded locally. The development of La Niña conditions can be seen in monthly SST anomaly maps (not shown) with the thin cool tongue first observed during spring, extending westwards from the eastern equatorial Pacific to its maximum extent of 170°E. Elsewhere in the

Pacific a warm, broad, but generally weak, asymmetrical 'V' shaped SST pattern surrounded the cool equatorial tongue, the southern arm extending across the Pacific to the South American coast. In the northwest Pacific monthly SST anomalies exceeded $+2^{\circ}\text{C}$ and warm anomalies of $+1^{\circ}\text{C}$ and above were located in the central northern and central southern Pacific. These anomalies were most prominent in February, the peak of this La Niña phase. Significant cool anomalies were found in the southeast, southwest and northeast Pacific.

In the Australian region the most visible feature was the area of very warm SSTs to the southwest of and along the Western Australian coast (Fig. 3). Local monthly anomalies to the southwest reached $+3^{\circ}\text{C}$. The anomalously warm waters in this region are reflected in the amplitude of the second EOF (Empirical Orthogonal Function) of SSTs used in the National Climate Centre's seasonal forecast prediction scheme (Drosowsky and Chambers 1998). The highest monthly value of this index during summer was in January 2000 with $+2.6$. This was the third highest month by value in a series since 1949 and is only slightly surpassed by values in the previous peak of the La Niña phase in early 1998 (Trewin 1999). A warming trend in this index has been observed since 1949 reflecting a general warming trend in the Indian Ocean SSTs (Drosowsky and Chambers 1998). It is also interesting to note that four out of the ten wettest Western Australian summers have occurred in the 1990s. Elsewhere around Australia there were weak warm SST anomalies,

Fig. 3 Anomalies of sea-surface temperature for summer 1999/2000 ($^{\circ}\text{C}$).



with the exception of cool anomalies along the east coast of Australia. Further south in the Southern Ocean and within the Antarctic circumpolar current a large negative SST anomaly matured over the latter part of the season. The resulting coupled effect is seen in the anomalously high anticyclonic MSLP in this region over summer (Fig. 7).

Elsewhere, in the northern Indian Ocean and around the majority of the Indonesian Archipelago weak positive SSTs were present. The southern Indian Ocean exhibits a dipole pattern with cool and warm SST anomalies in the southwest and southeast respectively with weak cool anomalies further south in the Southern Ocean.

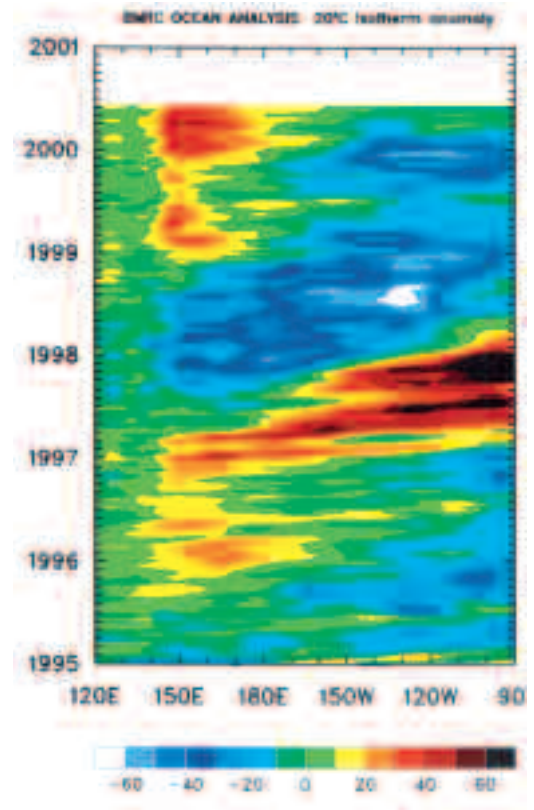
Subsurface ocean patterns

Figure 4 shows the Hovmöller diagram for the 20°C isotherm depth anomaly across the equator from January 1995 to June 2000. The 20°C isotherm depth is generally situated very close to the equatorial ocean thermocline, the region of greatest temperature gradient with depth and the boundary between the warm near-surface and cold deep ocean water. Negative anomalies indicate a shallower mixed subsurface layer and are associated with cool equatorial SSTs.

The redevelopment of La Niña conditions is evident as a shallowing of the 20°C isotherm depth in the eastern equatorial Pacific (Watkins 2000; Jones 2000) since August 1999. In January the shallow anomaly peaked at -50 m between 140°W-110°W. On this basis subsurface La Niña conditions had reached maturity. Meanwhile, over summer, the Western Pacific subsurface shows a deepening of the thermocline, indicating a warmer and mixed layer.

Intraseasonal variability of the subsurface is shown in Fig. 5 by a sequence of equatorial Pacific vertical temperature profiles from November 1999 to February 2000. Over summer the eastern Pacific cool subsurface anomalies diminished in magnitude and depth. The area of cool subsurface water in this region was greatest in December, however the strongest anomaly centred at around 100 m and 130°W occurred during January. Again, the subsurface temperature profiles suggest that the La Niña had in fact reached maturity over December and January. The Western Pacific warm subsurface temperature anomalies increased and progressively undercut the cool central Pacific subsurface waters, which in turn, led to a strong temperature gradient with depth and cooler SSTs in the central western Pacific. It is interesting to note that during February the 150 m depth-averaged temperatures (not shown) in the far eastern equatorial Pacific showed a slight warming, however the asymmetry of this anomaly about the equator suggests that it was due to local circulation anomalies.

Fig. 4 Time-longitude section of the monthly anomalous depth of the 20°C isotherm at the equator for January 1995 to early June 2000. Contour interval is 10 m.

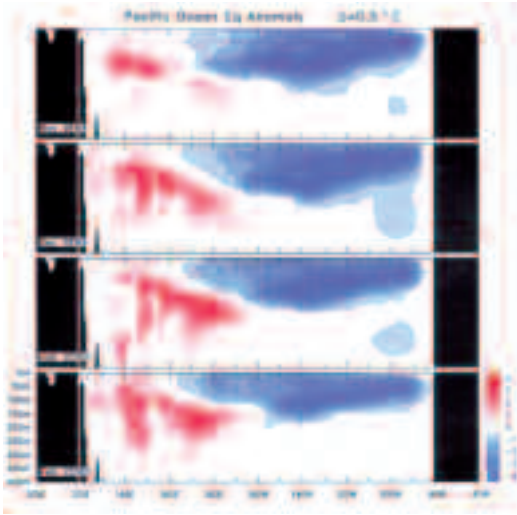


Surface analyses

The southern hemisphere summer 1999/2000 MSLP pattern is shown in Fig. 6, with the corresponding anomaly pattern provided in Fig. 7. These anomalies are the difference from an eleven-year (1979-89) climatology obtained from the European Centre for Medium Range Weather Forecasts (ECMWF).

The most notable changes in the summer MSLP pattern (Fig. 6) from the previous (spring) season (Watkins 2000) was the eastward and southward progression of mid-latitude high pressure in the central Indian, western Pacific and eastern Atlantic. In the higher latitudes the Antarctic circumpolar vortex became increasingly zonal and climatologically the polar high diminished in intensity. Over Australia a west coast trough and east coast ridge were dominant features.

Fig. 5 Four month November 1999 to February 2000 sequence of vertical temperature anomalies at the equator. Contour interval is 0.5°C.



The resultant MSLP anomaly distribution (Fig. 7) shows the eastward movement of high pressure in the Indian, Pacific and Atlantic Oceans, with a well-structured wave number three pattern and maxima centred around 50°S at longitudes 130°E, 25°W and 115°W respectively. The anomalous high pressure in the Australian region, a feature of the previous seasons (Watkins 2000; Jones 2000) remained during summer, with a ridge positioned along eastern Australia strengthening to +4 hPa. Another area of interest is a weak low MSLP anomaly appearing in the eastern Indian Ocean, off the northwest coast of Australia. Low MSLP anomalies in this region are associated with a positive SOI (Jones and Trewin 2000) and increased cyclonicity and correlate highly with all-Australian rainfall (Leighton et al. 1997).

Intraseasonal MSLP, anticyclonicity and cyclonicity anomaly patterns (not shown) in the Australian region show that areas of abnormally high MSLP and anticyclonicity were approximately five degrees south of their climatological positions (Jones and Simmonds 1993; Leighton 1993). In December anomalous high MSLP was positioned well south, around 50°S, off the southwest of Western Australia and a deep trough formed on the Western Australian coast. Cyclonicity maxima appeared in the Timor Sea and extended over the Pilbara region of Western Australia. These anomalies were due mostly to tropical cyclones *Ilsa* and *John*, which both crossed the Pilbara coast mid December and subsequently brought widespread rain to the region. Positive differences of July-September

Fig. 6 Mean sea-level pressure for summer 1999/2000 (hPa).

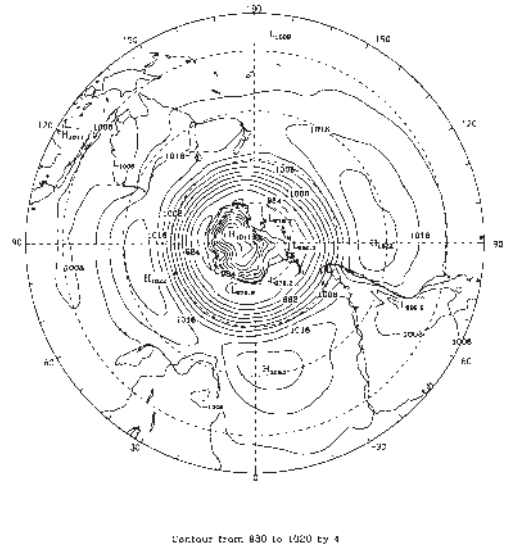
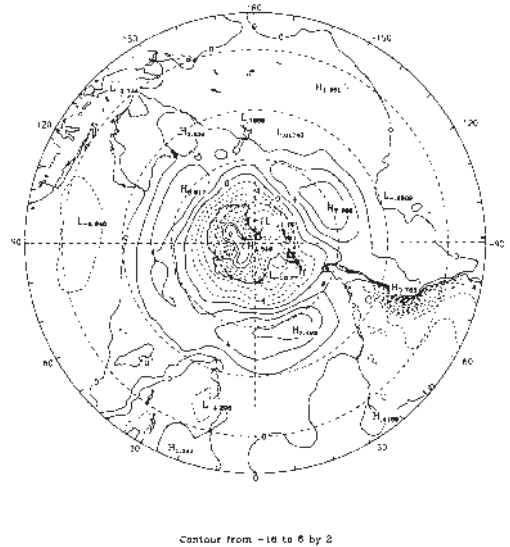


Fig. 7 Anomalies of the mean sea-level pressure from the 1979-89 European Centre for Medium Range Weather Forecasts climatology, for summer 1999/2000 (hPa).



averaged SOI in the current year minus those of the previous year have been linked to an increased likelihood of early season tropical cyclones crossing the northwest Australian coast (Broadbridge and Hanstrum 1998). Summer 1999/2000 was inconsistent with this relationship in that this difference was negative (-9.4) and two early season coastal crossings occurred during this month. January saw the migration of the high MSLP anomaly eastwards to a position south of Tasmania with its centre just south of 50°S. In

January, two areas of maximum anticyclonicity were located west (132°E) and east (160°E) of the high MSLP anomaly and around 43°S , well south of climatology (Leighton 1993), but located in positions which are typical for a positive summer SOI (Nowak and Leighton 1997). An interesting feature was a ridge of high pressure that formed between these two centres and extended over eastern Australia. This resulted in below average January rainfall in the eastern half of the continent and some lowest on record totals in northern New South Wales. By February the anomalously high MSLP moved east and north into the central Tasman Sea favouring cooler than normal SSTs. Centres of high cyclonicity returned to the Kimberly, Timor Sea and the Coral Sea. Tropical cyclone *Steve* formed late in the month in the Coral Sea and after crossing the Queensland coast followed an extraordinary path around the continent.

Mid-tropospheric analyses

Figures 8 and 9 show the mean and anomalous summer 1999/2000 500 hPa geopotential height patterns respectively. In general, the mid-troposphere exhibited an extremely zonal circumpolar vortex and (equivalent) barotropic pattern. A similar three-wave structure evident in the surface pressure pattern (Fig. 7) was also seen in the mid-levels. Anomalously high geopotential heights were positioned around 50°S at 130°E , 25°W and 115°W (Fig. 9). Trenberth and Mo (1985) note that major blocking episodes in these areas are associated with wave number three patterns.

Two significant low geopotential height anomalies, one in the Ross Sea and the other in the Weddell Sea, also remained stationary relative to their MSLP anomalies (Fig. 7). It is worth noting that in the summer of 1998/1999 (Trewin 1999) a similar barotropic pattern between the surface and mid-levels existed, however the anomalously high geopotential height in the Australian region was situated further east.

Intraseasonal monthly anomaly geopotential heights (not shown) show the same zonal movements as their surface counterparts. A prominent blocking pattern was evident in January between anomalously high geopotential heights south of Tasmania and low heights in the central Tasman Sea. The three-wave pattern showed signs of changing to a higher mode during February.

Blocking

Figure 10 shows the daily Hovmöller Blocking Index (BI) for summer 1999/2000. The BI is a measure of the zonal 500 hPa flow at mid-latitudes relative to that at subtropical and high latitudes.

Fig. 8 Mean 500 hPa geopotential heights for summer 1999/2000 (gpm).

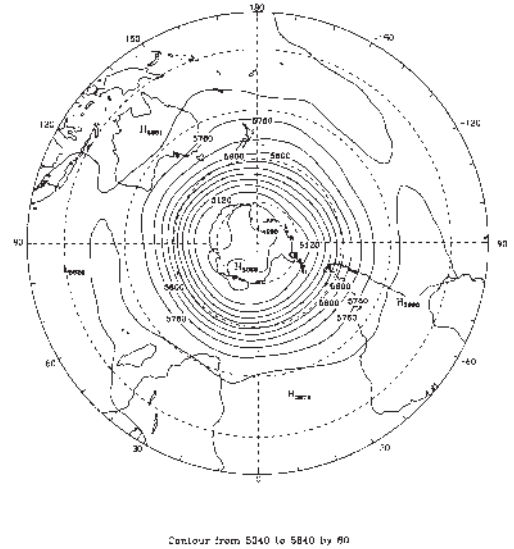
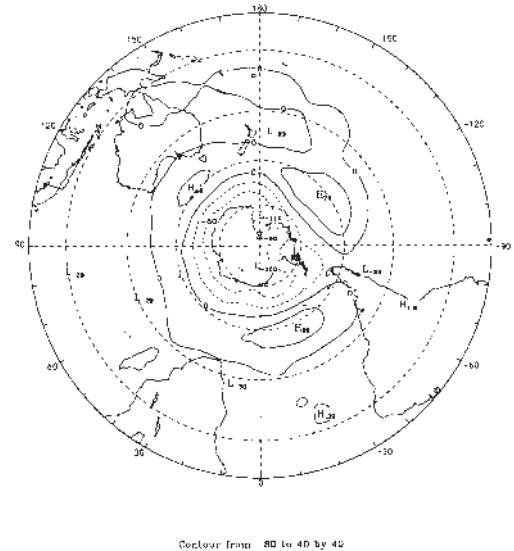
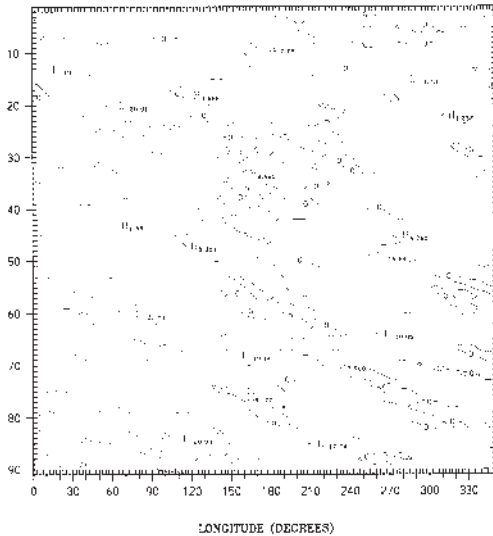


Fig. 9 Anomalies of the 500 hPa geopotential height from the 1979-89 European Centre for Medium Range Weather Forecasts climatology, for summer 1999/2000 (gpm).



During summer 1999/2000 the major blocking episodes occurred between the longitudes 150°E and 150°W , with more blocking in the Australian region during late December and early January. This is the climatologically preferred area of blocking in summer (Wright 1993; Trenberth and Mo 1985), however the 1999/2000 season exhibits abnormally high values of this index.

Fig. 10 Summer 1999/2000 daily blocking index: time-longitude section. Day 1 is 1st December 1999.



The blocking in the Australian region during early January shown in Fig. 10 failed to have a significant impact upon eastern Australian rainfall totals, however a cold outbreak led to cool maximum and minimum temperatures in the southeastern States and southern Queensland. Averaged over the month, the blocking pattern manifested itself on the surface as a broad ridge over eastern Australia and consequently did not lead to moist onshore flow to the southeast Australian coast.

Low and upper-level winds

Figures 11 and 12 show the low-level 850 hPa and upper-level 200 hPa wind anomalies for summer 1999/2000. These anomalies are with respect to an eleven-year ECMWF climatology.

Low-level wind anomalies in the western and central equatorial Pacific show enhanced easterlies fed by strong northeast trades in the eastern equatorial Pacific. These are consistent with an enhanced Walker circulation, and a zonal equatorial SST temperature gradient (Fig. 3). Strong equatorial westerly flow over the Indian Ocean also fed the enhanced convective activity over Indonesia and northern Australia. In the southern hemisphere subtropics, anticyclonic wind anomalies correspond to surface MSLP anomaly patterns (Fig. 7). Further south, highly zonal westerlies encircled Antarctica.

Over summer, Australia was dominated by northerly flow, strongest over western and central

regions. Cyclonic winds were present off the north-west coast of Western Australia. To the south, a broad band of easterly anomalies stretched from 140°E to 60°E. In the southern Tasman Sea a weak anticyclonic pattern was observed with mostly diffluent flow found elsewhere along the east coast of Australia.

In the upper levels (Fig. 12) strong westerly anomalies were found over the central and eastern equatorial Pacific, while strong southeasterly upper winds dominated the equatorial and northern Indian Ocean. Over Australia, enhanced southerly flow existed over the eastern half of the continent. In February this flow was more easterly, a phenomena associated with an enhanced monsoon (Trewin 1999; Drosowsky 1996). Further south a well-organised polar jet stream encircled most of Antarctica.

Australian region

Rainfall

National rainfall totals for the summer of 1999/2000 and an associated decile analysis, based on the post-1900 period are shown in Figs 13 and 14 respectively.

The majority of Australia received above average rainfall over summer, with some parts of western and central Australia receiving their highest rainfall totals on record. Australia received its third highest summer total rainfall and Western Australia recorded its wettest summer since records began in 1890 with an areal average of 325 mm. Normal to dry conditions were experienced in central Tasmania, along the central New South Wales coast and in the northeast of the State, along with parts of southeast Queensland.

During December most of the country experienced above average rainfall totals. In the western half of Australia major system influences included an active west coast trough and the coastal crossing of two tropical cyclones. Severe tropical cyclone *John* (category five) formed in the Timor Sea and followed a southerly track bringing widespread heavy rain to the Pilbara coast with the subsequent rain depression moving inland and flooding the Pilbara region. Wittenoom recorded the State's highest daily total of 302 mm on 16 December. Tropical cyclone *Ilsa* formed in the Indian Ocean, and generally followed a southeasterly track to cross the Pilbara coast as a category one cyclone two days after *John*, but failed to produce much significant weather. Central Australia also felt the effects of cyclone *John*. Parts of southwest Northern Territory and northwest South Australia received very much above average totals. The interaction of a slow-moving surface trough and unstable tropical air from the northeast triggered extensive thunderstorms across South Australia earlier in the

Fig. 11 Anomalies of the vector wind at the 850 hPa level from the 1979-89 European Centre for Medium Range Weather Forecasts climatology, for summer 1999/2000 ($m s^{-1}$).

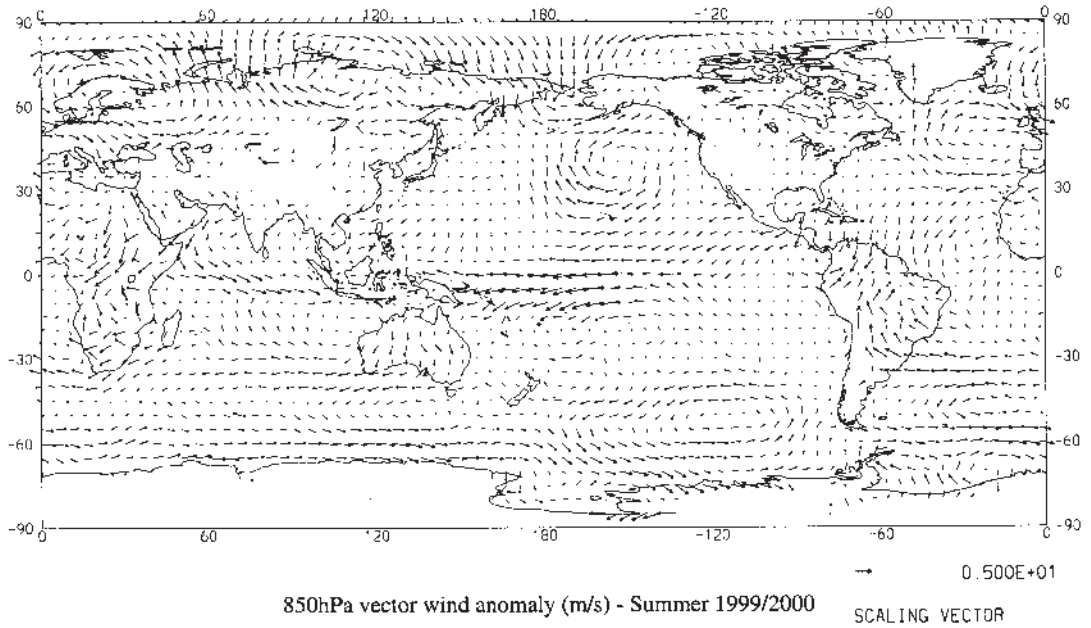


Fig. 12 Anomalies of the vector wind at the 200 hPa level from the 1979-89 European Centre for Medium Range Weather Forecasts climatology, for summer 1999/2000 ($m s^{-1}$).

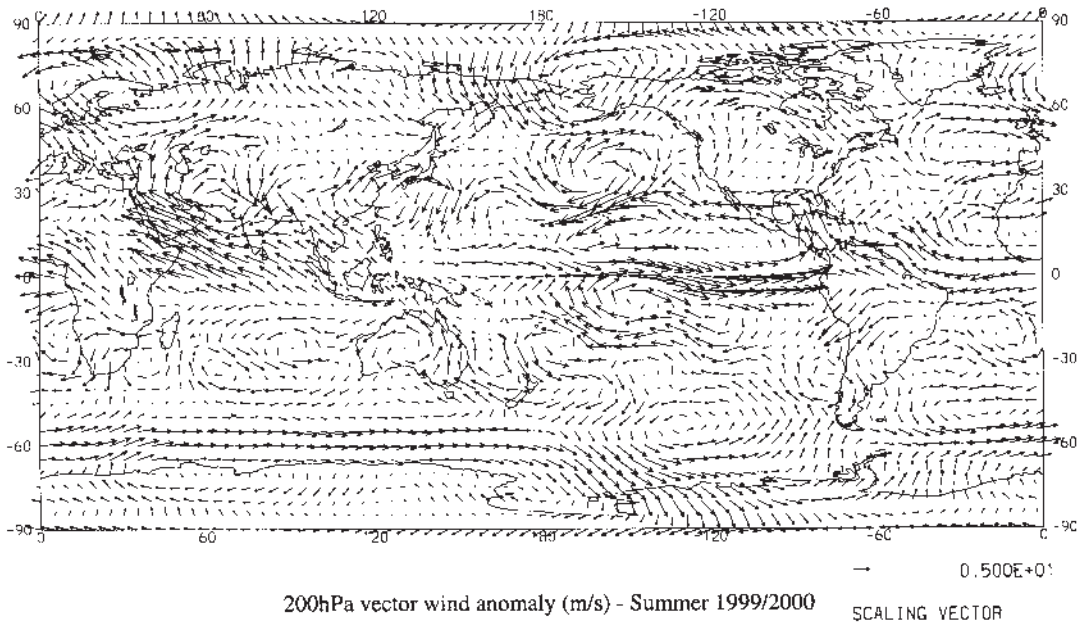


Fig. 13 Rainfall totals over Australia for summer 1999/2000 (mm).

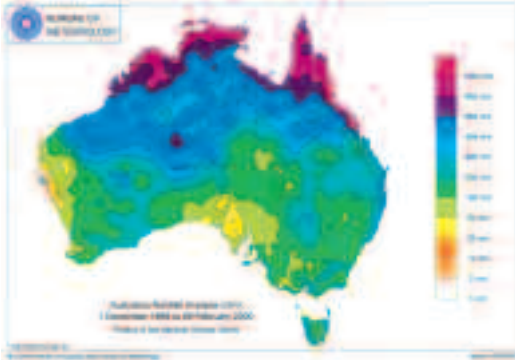
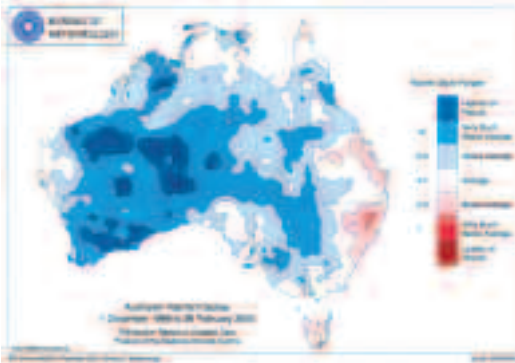


Fig. 14 Deciles of rainfall over Australia for summer 1999/2000, based on 100-year 1900-99 base period.



month, with a severe storm developing over Eyre Peninsula which dissipated five hours later near the South Australian/New South Wales border. Flooding occurred in western Queensland and New South Wales. Wilcannia received its highest monthly total on record with 252.3 mm when a series of surface and middle level troughs and frontal systems interacted. A low pressure system off Queensland's northern coast produced above average rain with some totals over 600 mm. Rainfall was below average in parts of western central Queensland and central Tasmania.

January rainfall figures showed wet conditions prevailed in the western half of the country with a substantially drier pattern in the eastern half of the continent compared to the overall summer pattern (Fig. 14). The main influences on the Western

Australia rainfall were the interaction of surface and middle-level troughs and moisture from tropical lows. Over the second half of the month, these interactions produced widespread thunderstorms about the southwest. Some localities within this region recorded their highest daily totals. A tropical low formed 350 km northwest of Darwin and tracked south, crossing the Pilbara coast. Local heavy falls in the order of 200 mm were recorded as it passed. The moisture from this low travelled southeast and interacted with a surface trough, bringing above average falls to southern Northern Territory and western South Australia. Average to below average falls were recorded over the northern half of the Northern Territory. Although the monsoon trough was present, it failed to produce extensive rain events. The eastern states were generally drier than average with some isolated lowest on record monthly totals around the western New South Wales/Queensland border. Synoptic analyses show the persistence of a surface ridge over the eastern States (Fig. 7). In Tasmania above average falls in the north and east were attributable to lows that developed in passing troughs early and late in the month. The highest monthly total was 398 mm at Gray.

The distribution of rainfall during February 2000 (not shown) displays an interesting spatial pattern of above average rainfall across central and northern Australia, and areas of below to well below average rainfall in south western Western Australia, southeast Queensland and eastern New South Wales. The wet areas were the result of a broad trough fed by moist tropical air. The dry west and east coasts were caused by passing highs ridging over both regions, maintaining a dry weather pattern. An extensive area of well above average rainfall occurred in central Australia with highest on record rainfall west and south of Alice Springs into Western Australia and northern South Australia. In central Queensland, Winton registered highest on record February rainfall with 463.8 mm. This rainfall was due to slow-moving low pressure systems in a persistent monsoonal trough. Coastal catchments were flooded in the area between Cooktown and Mackay, recording well above average rainfall for the month. Synoptic analyses point to moist airflow from the Coral Sea converging with the monsoon trough resulting in the formation of tropical cyclone *Steve* later in the month. Southeast Queensland and northeast New South Wales experienced dry conditions as a ridge extended from a dominant high in the Tasman Sea. In western New South Wales, rainfall was also well above average with highest on record monthly totals located in the northwest of the State around Wilcannia. This rainfall also extended to northwest Victoria and southeast South Australia.

Temperatures

Figures 15 and 16 show the maximum and minimum temperature anomalies over Australia for summer 1999/2000. Maximum temperatures were well below average across most of the country. Western Australia recorded its coolest summer conditions since 1950 with a state-averaged maximum temperature anomaly of -2.1°C . Notable exceptions to the below normal maximum temperature conditions included positive anomalies along the western Western Australian coast and a band across southern South Australia, Victoria and Tasmania. Figure 15 is a typical distribution of maximum temperature anomalies for a positive SOI phase (Jones and Trewin 2000). Minimum temperatures were mainly below average. Two significant regions of cooler than average minimum temperatures existed, one in central and northern Western Australia and the second a broad band of cooler than average minimum temperatures stretching from eastern Northern Territory to the mid Queensland and southern New South Wales coast. Areas of higher than average minimum temperatures occurred along the Western Australian coast around Shark Bay and the southern half of South Australia. This pattern in minimum temperatures is also typical of a positive SOI phase (Jones and Trewin 2000).

Both December maximum and minimum temperature anomaly maps (not shown) look similar to the overall summer patterns. The persistent northeasterly flow resulted in maximum temperature anomalies along the west coast in the order of 2°C to 4°C above the 1961-1990 long-term average. Central Western Australia, southwest Queensland and northwestern New South Wales experienced the coolest maximum temperatures with monthly anomalies of up to 5°C below the long-term average. The areally averaged December maximum temperature anomaly for New South Wales was the coolest on record with -2.6°C . Minimum temperatures were also below average over most of the country, with the coolest anomalies in eastern central Western Australia, southeast Queensland and northeast New South Wales. A new Australian December minimum temperature record of -7.0°C was recorded at Charlotte Pass.

Western Australia continued to show below average maximum and minimum temperature anomalies during January, a result of the increased cloudiness and rainfall in the area. The Western Australian January maximum temperature anomaly was the coldest since the start of records in 1950. Cooler than average minimum temperatures in central and northern New South Wales and southern central Queensland were partly due to a cold outbreak later in the month, a function of the blocking pattern (Fig. 10).

Fig. 15 Summer 1999/2000 maximum temperature anomalies ($^{\circ}\text{C}$) for Australia based on a 1961-90 mean.

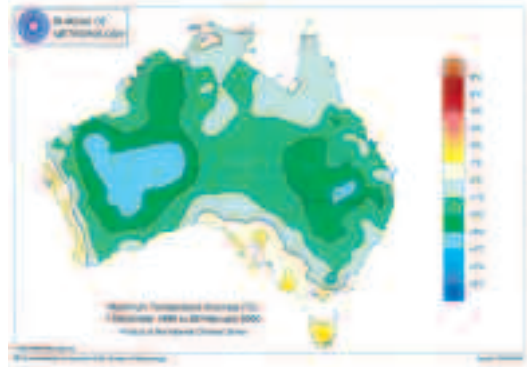
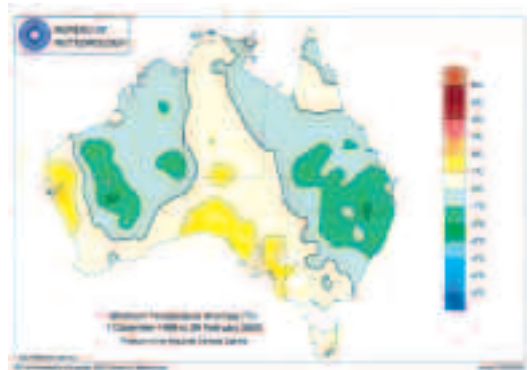


Fig. 16 Summer 1999/2000 minimum temperature anomalies ($^{\circ}\text{C}$) for Australia based on a 1961-90 mean.



In February, the peak of this La Niña phase again shows a characteristic pattern of maximum temperature anomalies consistent with a positive SOI (Jones and Trewin 2000). Cooler than average temperatures in the northern half of the country contrasted with a warmer southern eastern Australia. Minimum temperature anomalies showed a similar pattern, however closer to average anomalies occurred in the northern half of Australia, except in far west Western Australia where Carnarvon recorded its highest ever February overnight minimum temperature of 30.0°C . Adelaide recorded its longest number of days above 30°C with 18 for the month, six days above the average. At the same time, Victoria experienced unusually hot weather, with the average February maximum for Melbourne of 30.1°C equalling the second highest

mean maximum temperature ever for February. Many places in Victoria and Tasmania had their hottest February on record, and there were several major bushfires in Tasmania.

Acknowledgments

The author would like to thank Bob Leighton (National Meteorological and Oceanographic Centre, Bureau of Meteorology) for useful discussions on seasonal cyclonicity and anticyclonicity analyses.

References

- Broadbridge, L.W. and Hanstrum, B.N. 1998. The relationship between tropical cyclones near Western Australia and the Southern Oscillation Index. *Aust. Met. Mag.*, 47, 183-9.
- Climate Prediction Centre (CPC) 1999. *Climate Diagnostics Bulletin, December 1999*. U.S., Dept. of Commerce, National Oceanic and Atmospheric Administration, Washington D.C., USA, 88pp.
- Climate Prediction Centre (CPC) 2000. *Climate Diagnostics Bulletin, February 2000*. U.S., Dept. of Commerce, National Oceanic and Atmospheric Administration, Washington D.C., U.S.A., 80pp.
- de Hoedt, G. 2000. Seasonal climate summary southern hemisphere (autumn 1999): a decline in weak cold episode conditions in the tropical Pacific. *Aust. Met. Mag.*, 49, 51-8.
- Drosowsky, W. 1996. Variability of the Australian summer monsoon at Darwin: 1957-1992. *Jnl Climate*, 9, 85-96.
- Drosowsky, W. and Chambers, L.E. 1998. Near global sea surface temperature anomalies as predictors of Australian seasonal rainfall. *BMRC Research Report no. 65*, Bur. Met., Australia.
- Jones, D.A. and Simmonds, I. 1993. A climatology of Southern Hemisphere extratropical cyclones. *Climate Dynam.*, 9, 131-45.
- Jones, D.A. 2000. Seasonal climate summary southern hemisphere (winter 1999): a return to near normal conditions in the tropical Pacific. *Aust. Met. Mag.*, 49, 139-48.
- Jones, D.A. and Trewin, B.C. 2000. On the relationships between the El Niño-Southern Oscillation and the Australian land surface temperature. *Int. J. Clim.*, 20, 697-719.
- Leighton, R.M. 1993. Monthly anticyclonicity and cyclonicity in the southern hemisphere 15 year (1973-1987) averages. *Technical Report 67*, Bur. Met., Australia.
- Leighton, R.M., Keay, K. and Simmonds, I. 1997. Variations in annual cyclonicity across the Australian region for the 29-year period 1965-1993 and the relationships with annual Australian rainfall. *Climate prediction for agricultural and resource management : Australian Academy of Science Conference*, Canberra, 6-8 May 1997, 257-67.
- Nowak, H. and Leighton, R.M., 1997. Relationships between east coast Australasian anticyclonicity, the Southern Oscillation and Australian rainfall. *Aust. Met. Mag.*, 46, 267-76.
- Trenberth, K. and Mo, K.C. 1985. Blocking in the Southern Hemisphere. *Mon. Weath. Rev.*, 113, 3-21.
- Trewin, B. 1999. Seasonal climate summary southern hemisphere (summer 1998/99): a weak cold event (La Niña) in the Pacific basin. *Aust. Met. Mag.*, 48, 285-93.
- Watkins, A.B. 2000. Seasonal climate summary southern hemisphere (spring 1999): a transition toward a second successive cool episode (La Nina). *Aust. Met. Mag.*, 49, 319-30.
- Wright, W.J. 1993. Seasonal climate summary southern hemisphere (autumn 1992): signs of a weakening ENSO event. *Aust. Met. Mag.*, 42, 191-8.

Appendix

The main sources for data used in this review were: National Climate Centre, *Climate Monitoring Bulletin - Australia*. Obtainable from: National Climate Centre, Bureau of Meteorology, GPO Box 1289K, Melbourne, Vic. 3001, Australia.

Climate Prediction Centre, *Climate Diagnostics Bulletin*. Obtainable from: Climate Prediction Centre, National Weather Service, Washington D.C., USA, 20233.

Numerical prediction model performance summary July to September 2000

W. Skinner and T. Hart

National Meteorological and Oceanographic Centre, Bureau of Meteorology,
Australia

(Manuscript received December 2000)

Introduction

This summary continues the series comparing the performances of numerical weather prediction (NWP) models.

Models and methods

A description of the Australian verification methods can be found in a previous article (Skinner 1995).

Models are from the National Meteorological and Oceanographic Centre (NMOC) Melbourne and from ECMWF (European Centre for Medium-range Weather Forecasts), NCEP (National Centers for Environmental Prediction), UKMO (United Kingdom Meteorological Office) and JMA (Japan Meteorological Agency).

Four models considered from NMOC, Melbourne, are: LAPS_PT375 (Limited Area Prediction System Point 375); MESO_LAPS_PT125 (MESOscale Limited Area Prediction System Point 125); TLAPS_PT375 (Tropical Limited Area Prediction System Point 375); and GASP (Global Assimilation and Prediction).

Overseas global models included in the comparisons are: ECSP (ECMWF Spectral Assimilation); USAVM (NCEP Spectral model for aviation); UKGC (UK Meteorological Office Grid PE model); and JMAGSM (JMA Global Spectral Model).

Very short summaries of the models can be found in the initial article (Skinner 1995) with references to model updates in subsequent issues.

All results have been calculated within NMOC Melbourne, where the models were verified against their own analyses. Results are presented for the irregular Australian verification area only (see Fig. 5).

The statistics are a measure of the skill in forecasting geopotential height at 500 hPa or mean sea-level pressure (MSLP). Other field types are not included in these summaries.

The limited area models are run several hours earlier than GASP and this premature data cut-off, particularly for satellite information, adversely affects their skill compared to GASP.

Note that the Australian region verification grid has southerly points which are outside the TLAPS_PT375 grid and easterly points outside the MESO_LAPS_PT125 grid. TLAPS_PT375 and MESO_LAPS_PT125 scores are calculated without these points and are therefore not strictly comparable with those from other models.

Notes on NWP systems

Acronyms

AMSU	Advanced Microwave Sounder Unit
ATOVS	Advanced TOVS
GTS	Global Telecommunication System
HIRS	High-resolution Infrared Radiation Sounder
MSU	Microwave Sounding Unit
NESDIS	National Environmental Satellite Data and Information Service (USA)
NOAA	National Oceanic and Atmospheric Administration (USA)
TIROS	Television Infra-red Observational Satellite
TOVS	TIROS Operational Vertical Sounder

Corresponding author address: Ms Wilma Skinner, National Meteorological and Oceanographic Centre, Bureau of Meteorology, GPO Box 1289K, Vic. 3001, Australia.